Journal of Techniques, ISSN: 2708-8383, Vol. 7, No. 1, 2025, Pages 80-93
DOI: https://doi.org/10.51173/jt.v7i1.2358

JOURNAL OF TECHNIQUES

Journal homepage: http://journal.mtu.edu.iq

RESEARCH ARTICLE - MECHANICAL ENGINEERING

Energy and Performance Analysis of Solar Solid-Dry Cooling Systems for Energy-Efficient Buildings in Tropical Regions

Saleh Radam Saal[1], Armaan Adamian[1], Ali Adelkhani[2*]

[1]Department of Mechanical Engineering, South Tehran Branch, Islamic Azad University, Tehran, Iran

[2]Department of Mechanical Engineering, Kermanshah Branch, Islamic Azad University, Kermanshah, Iran

[*] Corresponding author E-mail: a.adelkhani@iauksh.ac.ir

Article Info.

Article history:

Received
27 January 2024

Accepted
11 June 2024

Publishing
31 March 2025

Abstract

In pursuing energy-efficient building solutions, renewable energy sources like solar power are increasingly utilized in ventilation and cooling systems. This study specifically investigates a solar-powered desiccant cooling system's performance against the traditional fan coil unit (FCU) in residential settings. It highlights the potential for energy savings and improved environmental outcomes. A model employing a solar heater with a vacuum tube is developed and simulated using TRNSYS to perform a critical thermal analysis of these systems. Key results show that increasing the input current to the collectors reduces the necessary collector area, thereby enhancing overall system efficiency. Energy evaluations reveal that the FCU, with a room moisture content of 79.4%, fails to provide adequate cooling due to its inability to meet the desired 45% moisture threshold. The drying process consumes the most energy, accounting for 38% of total usage. However, the solar hybrid dehumidifier cooling method demonstrates economic efficiency, achieving 18.4% in structures with high residual loads. Ambient temperatures and moisture content are effectively lowered to 24.8 – 25 °C, and 63%–67%, respectively, using the two-phase solar dehumidifier cooling device. This adjustment leads to 28.7% and 34.6% energy savings for convection and recirculating options. These findings underscore the potential of solar-powered systems to enhance energy efficiency and reduce environmental impacts in tropical climates.

Publisher: Middle Technical University

Keywords: Energy; Solar; Solid-Dry; Cooling Systems; Buildings.

1. Introduction

Renewable electricity ventilation mechanisms optimize home ventilation to minimize energy waste [1]. In winter, the air is heated by transferring heat from the warm interior to cooler incoming air using energy wheels, often containing silica gel, reducing heating costs. In warmer months, the warmer interior air cools the incoming air, saving on cooling expenses. The eco-friendly fan and engine system can be powered by solar energy [2]. A sunlight-powered chimney uses airborne condensation to direct airflow downwards, with forced convection transforming it. A waterfall effect, created by mixing water with a dehumidifier like calcium chloride, dehumidifies the space [3]. This system uses solar power to replenish fluids and a low-speed water machine for transport, aiming for low energy use and continuous operation in solar thermal dehumidification.

Dynamic solar heating uses rooftop solar thermal collectors to power the cooling system of a dryer [4]. Affordable systems employ airflow over desiccant-impregnated substances for drying and air rejuvenation. Solar radiation fuels regeneration, while packed towers, though not widely used commercially, offer countercurrent air and liquid desiccant flow. Research shows air preparation enhances dehumidifier renewal [5]. Properly packed, an insulated column acts as a humidifier/regenerator, minimizing pressure loss. This method uses solar thermal power to create a low-temperature environment without active cooling. Solar construction aims to reduce heat escape in summer, enhancing excess heat removal. This involves understanding heat conduction and solar radiation.

A significant portion of a building's energy is used for air conditioning, which relies heavily on fossil fuels to generate electricity, leading to increased greenhouse gases, especially carbon dioxide [6]. This exacerbates environmental issues. Therefore, using renewable energy and developing clean, efficient, and eco-friendly technologies is essential to reduce energy consumption and the construction industry's carbon footprint while ensuring optimal living conditions. It is essential to use renewable energy and develop clean, efficient, and eco-friendly technologies [7].

Among these methods, the cooling-drying technique emerges as a promising solution. Researchers are studying these devices to improve performance and minimize environmental impact. The exploration of cooling-drying techniques began in 1930 and has continually evolved [8]. Dehumidifier cooling technologies offer energy-efficient and environmentally friendly climate control. They improve indoor air quality and control latent heat, efficiently using low-grade energy sources like solar waste and electrical heat.

Nomenclature & Symbols			
TSDCS	Two Stage Desiccant Cooling System	OSDCS	One-Stage Desiccant Cooling System
HDCS	Hybrid Desiccant Cooling System	HVAC	Heat Ventilation and Air Conditioning
FCU	Fan Coil Unit	COP	Coefficient of Performance
VC	Vapor Compression	FEA	Finite Element Analysis

Using sunlight to generate heat is an appealing option for thermal dehumidifier cooling ventilation to minimize environmental impact. Dryer cooling structures have two air flows: the initial stream supplies air to the ventilated area, and the subsequent stream replenishes the desiccant layer. The key processes in desiccant cooling systems—dehydration, refrigeration, and moisture addition—aim to provide cooled and dehumidified air to the room. A comprehensive literature review in this thesis explores the operational theory of drying systems, temperature and solar-assisted drying systems for cooling, and evaporative coolant systems based on existing literature [9]. As a result, multiple dry evaporative air-cooling systems were examined.

The hypothesis is to determine if all environmental conditions can be obtained from standard sources like TRNSYS software. Solid desiccated cooling structures (SDCS) are identified as effective for managing dehydration and chilling in two sections of the chemical dehydrator and chilling device. The solid rotational drying wheel (DW) and heating source in the chemical dehydrator benefit from waste heat and solar power. Chemical dehumidifying uses adsorbent substances to absorb and release water molecules using thermal energy, unlike mechanical dehumidifying, which uses cooling energy to condense water molecules [10].

According to the cooling process, a desiccant conditioning system's designs can be separated into evaporative and composite types. After the dehumidifying step, a cooler that evaporates water is used in an evaporative drying system for cooling. In a hybrid dehumidifier cooling structure (HDSC), a chilled-water system or vacuum air conditioner (VAC) is employed as a device for cooling after the chemical-based dehydrating procedure. Various locales have led investigators to build different versions of the dehumidifier air conditioner. In [11], the effectiveness of an investigational one-stage evaporated dehumidifier air conditioner (OSDCS) for three distinct environments was assessed. Their findings demonstrated that in a hot and muggy environment, a single-stage evaporating dehumidifier conditioning process in isolation from any additional cooling equipment was unable to meet the requirements for comfort in the interior. The second-stage dehumidifier air conditioner (TSDCS), which includes two exchangers for heat before the conditioning equipment and an additional dehydration procedure, was suggested in [12]. The effectiveness of a TSDCS has been extensively assessed in three distinct outdoor circumstances as an indicator of regenerated temperatures (60 ◦C to 110 ◦C). They discovered that although the system's percentage of efficiency (COP) is dependent on regenerated temps and external circumstances, the TSDCS could manage the cooling demands of a structure in a different environment. The effectiveness of TSDCS combined with expanded tube-shaped solar air collection systems in the country's hot and humid climate was assessed in [13]. According to their findings, the equipment's COP could approach one when the source of air was at roughly 18 °C, or 60%. Because the TSDCS requires far lower renewal temperatures than the OSDCS, it has a substantially greater coefficient of performance (COP) than the OSDCS. To increase COP and the possibility of energy savings in the TSDCS, multiple investigations have been carried out. In [14], a simulation of several regeneration techniques led to a 15.5% increase in COP. [15] examined how well TSDCS performed with two different kinds of desiccant materials. They concluded that, at an elevated inlet air temperature, the TSDCS, with the addition of sodium polyacrylate, has a COP value that is 1.3–1.4 times higher than that of the silica gel. The efficiency of immediate evaporative cooling varies with climate, therefore while the COP and cost-effective advantages of TSDCS can be created based on operational circumstances, its application is environment-dependent. Due to its advantages over typical chilling systems used in humid and hot environments, including energy savings and temperature management, HDCS has become a competitive option in recent years. By integrating chemical dehumidifying with different chilling technologies, such as vacuum compression systems (VC) [16], split units [17], cooled ceilings [18], and chillers [19], several models and experimental experiments created HDCS. In a study focused on energy conservation, In [20] conducted an experimental study of the combination of solid adsorbent with an R407 splits unit in Egypt's hot and muggy climate. When comparing the air conditioner's electrical usage to the traditional split unit system, they discovered a 10.2% decrease. TRNSYS was created to assess how operating factors affected the system's efficiency. They showed how the system's COP is highly responsive to changes in the general humidity ratio and regenerative temperatures.

Three HDCS and TSDCS designs (TSDCS-V and TSDCS-R) were evaluated as potential FCU replacements in a conference room under Iraq's hot, humid conditions. An energy inspection assessed FCU efficiency, power distribution, and the impact of mechanical humidity reduction on electricity use and thermal comfort. The dehydration process consumed significant energy, and the FCU failed to meet temperature comfort requirements. Three solar dehumidifier air conditioning systems were developed and tested in TRNSYS based on cooling needs and dehumidifying capacity for an educational room. Outcomes were determined using predetermined performance markers. Metrics like temperature, COP, solar fractions, energy conservation, and CO2 emissions were considered to evaluate the three proposed cooling structures. This study aims to enhance the efficiency of solar desiccant cooling systems through the numerical simulation of a solar heater using a vacuum tube. The primary objective is to design an optimal model of the solar heater, conduct meshing, and apply necessary boundary conditions for a comprehensive thermal analysis. The research focuses on evaluating the impact of the solar heater on temperature outcomes, heat transfer, and heat flux to determine its effectiveness in supporting desiccant cooling systems. By integrating these findings, the study seeks to advance the development of sustainable, energy-efficient cooling technologies that reduce the environmental footprint, enhance indoor air quality, and contribute to more efficient energy use in building environments.

2. Related Work

Various air-cooling techniques can be employed to decrease the essential air load (the climate). These include organic processes like cooling by evaporation, heat transfer with cold water, and the utilization of heat engines (hybrid technology). There are two distinct categories of evaporation processes. Straight evaporative cooling methods involve humidifying the air to cool it before blowing it into the areas, while indirect evaporation systems use an air/air converter to just chill the air without humidification. These cooling devices can be used either directly, by raising moisture, or secondarily, by exchanging useful heat between primary and secondary air. Thus, the extraction method relies on both sensible and latent heat transmission.

The fundamental concept behind evaporative cooling is the direct transformation of thermal energy into hidden heat. Fig. 1 displays a psychrometric curve illustrating the efficiency of an indirect cooling by evaporation unit. In direct-impact cooling caused by an evaporation system, the air directly interacts with a humid setting, a fluid surface, or sprays [11]. The fundamental idea of this system is to lower the temperature of the fresh air by facilitating the evaporation of water. The water evaporates and releases its latent heat into the air stream. The transmitted energy is utilized to lower the air's Fahrenheit (dry bulb temperatures), resulting in a rise in humidity. This process occurs under conditions of constant temperature. The minimum attainable temperature equals the damp bulb's temperature of the initially delivered air [12]. The efficacy of direct cooling by evaporation is determined by calculating the ratio between the actual decrease in dry bulb temperatures and the highest possible decrease that can be achieved by lowered dry bulb temperature [13]. Camargo [14] undertook theoretical and laboratory studies of a direct evaporation air conditioning unit to assess its performance. This assessment was based on the formulas of energy, head, and transmission of mass. Fig. 2 depicts a schematic representation of the operational process of this direct-evaporation cooling unit. The obtained equation allows us to determine the effectiveness of direct evaporative cooling. They also concluded that evaporative cooling systems have great potential for thermal comfort relief and can still be used as an alternative to conventional systems in many tropical regions, saving energy and protecting the environment.

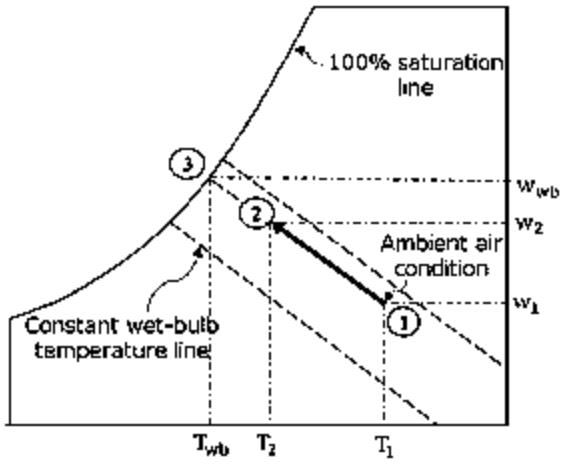

Fig. 1. Working principles (psychometric chart) of a direct evaporative cooling unit [13]

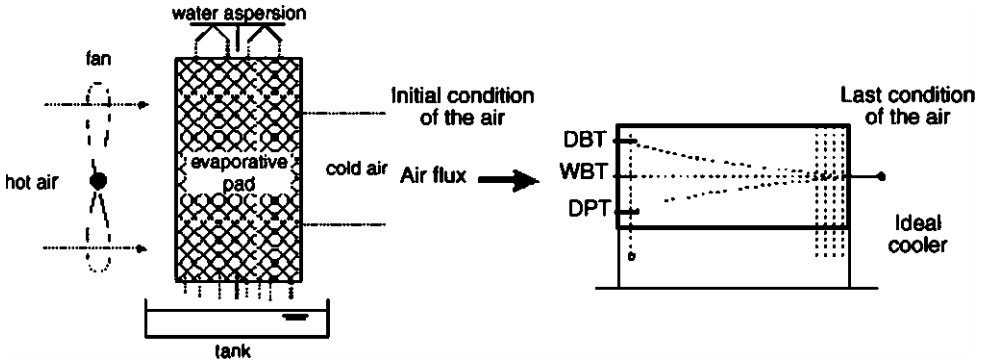

Fig. 2. Schematic of the functional mechanism of a direct evaporative cooling unit [10]

Indirect evaporative cooling uses an evaporative heat exchange system, such as a tube thermal exchange, plate heat converter, or rotary heater, to cool air without adding moisture. This method combines evaporation with a heat exchanger to deliver chilled air to the air source. The process cools the air without direct contact between the hydrated, cooled air and the supply air, maintaining lower temperatures than the wet bulb without adding extra moisture. Figs. 3 and 4 illustrate these changes in moisture and temperature: Fig. 3 shows an indirect air conditioning system's curve. The efficiency of these systems ranges from 70% to 80% [15], and they are especially effective in hot, arid climates like Kuwait [16]. Fig. 4 diagrams an intermediate cooling unit, while Fig. 5 shows a combined direct and indirect evaporative system [17]. This setup includes a humidifying arrangement known as the combined humidity control mode, potentially leading to high indoor dampness. Studies, including that of Jodi et al. [18] on variable loads in Iraqi homes, demonstrate evaporative cooling's effectiveness in maintaining a comfortable indoor environment. However, its performance is limited in humid or high-heat conditions, leading to the integration of desiccant dehumidification to manage the latent load and improve climate adaptability. This combined desiccant-evaporative system can achieve lower temperatures, as shown in Fig. 4 diagram of the operational procedure.

In drying structures, the drying process supplies the absorbed load, and direct and/or downstream evaporative cooling provides the sensible load, as shown in Figs. 5 and 6 [19]. Dehumidifying is a physical process where water molecules are trapped on the porous and granular surfaces of the adiabatic absorbent in cooling desorption and dehydration. The desiccant removes moisture from the air by creating a low vapor pressure area on its surface [19]. Water molecules move from the wet air to the drying desiccant due to the air's higher relative pressure and the desiccant's reduced vapor pressure. This process dehumidifies the air. Once saturated, the absorbent releases water when heated. Thermal power for reconditioning can come from electricity, waste heat, or solar collectors. Unlike mechanical refrigeration, the desiccant cooling system directly

generates fresh air. Fig 7 shows the operational principles of a refrigeration system for a dryer. The desiccant cooler comprises a dehydrator (desiccant unit), a regeneration heat source, and an evaporator unit (radiator, compressor, or cooling coil). In an evaporative heating and dryer system, clean air (ambient or mixed with return air) passes through the desiccant, converting latent heat to sensible heat. The air is then chilled in the compressor using a rotary heater and/or indirect condensation before entering the controlled area at optimal thermal comfort. During renewal, return air passes through a processing device and a rotating heat exchanger, then is heated and passed through the dehydrator to remove moisture from the dry absorbent. Fig. 5 shows this cycle. Camargo et al. [20] examined a standard setup of a drying cooling apparatus combining natural and recirculated air, demonstrating the effectiveness of linking the desiccant dehydrator with the evaporator cooling system.

Several studies have explored the design, concept, development, and evaluation of dry cooling structures [21]. Factors such as climate, equipment efficiency, operational conditions, drying wheel speed, air flow rate, and regenerating temperatures can influence the efficiency of dryer cooling systems. Research shows these systems can maintain comfortable temperatures in humid regions [22]. Modeling studies suggest that environmental conditions, demand dynamics, and the type of regenerating energy source affect the performance and economic viability of drying cooling devices, potentially enhancing their efficiency from 50% to 120% [23]. In absorbent cooling devices, humid air is cooled to a consistent humidity using a heat exchanger, with the remaining heat used to reactivate desiccants, boosting the coefficient of efficiency [24]. Studies indicate that increasing reactivating temperatures and external humidity improves dehumidification, visible energy ratio, and drying effectiveness [25]. A hybrid system at Central Queensland University showed a peak coefficient of effectiveness of 0.83, reducing energy consumption by 18% [26]. Researchers developed a solar-powered desiccant cooling device with a single rotor of six stages, demonstrating its effectiveness in lifetime cost, moisture elimination, thermal expansion, and dehumidifying.

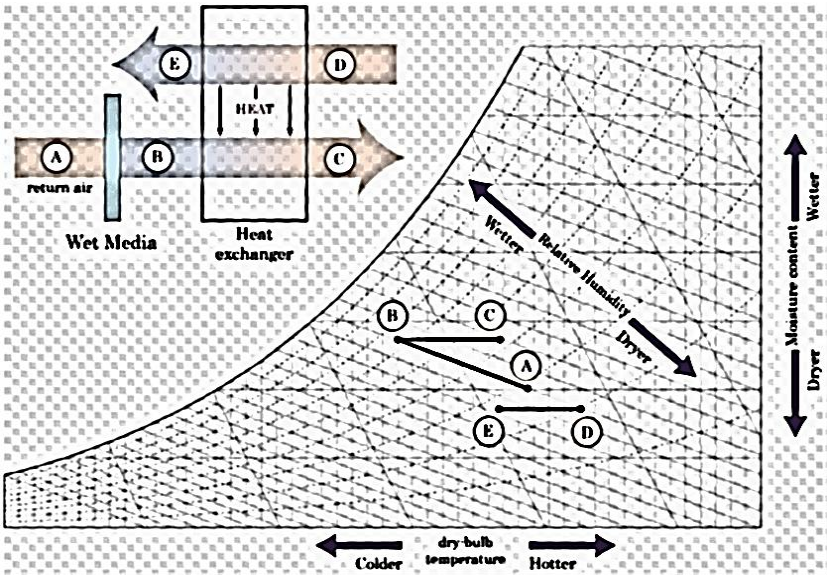

Fig. 3. Working principles (psychometric chart) of an indirect evaporative cooling unit [13]

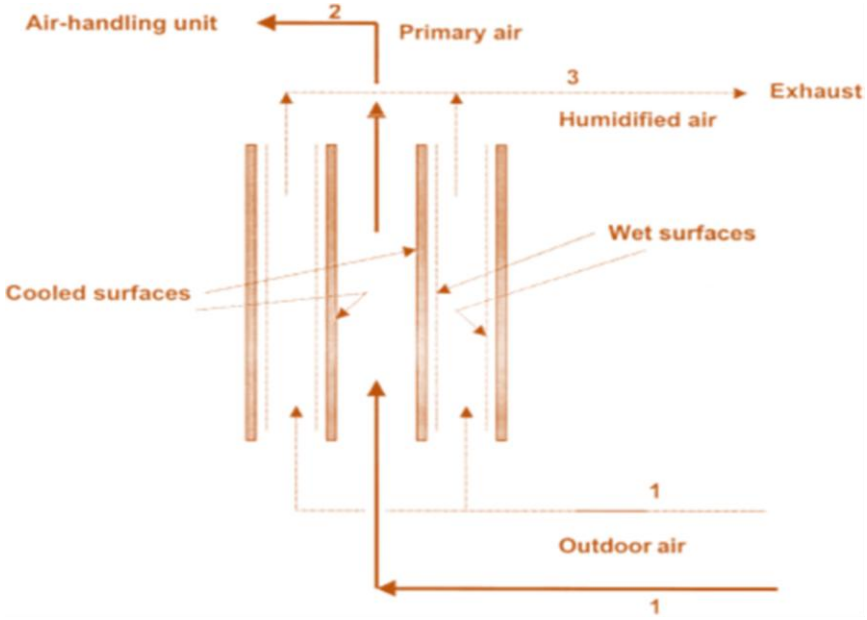

Fig. 4. Schematic of indirect evaporative cooler [14]

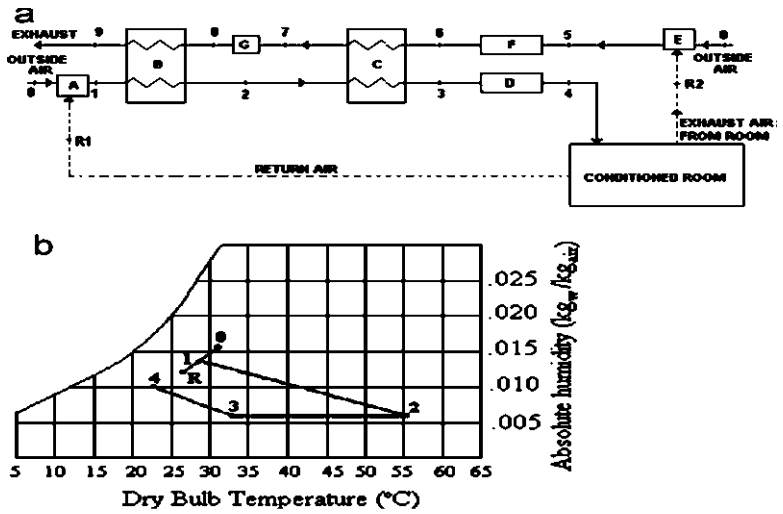

Fig. 5. a) cycle of the evaporative cooling system of the dryer; (A) mixer and process air fan, (B) dehumidifier dryer (rotary wheel), (C) energy conservation wheel, (D) direct evaporative cooling, (E) mixer and reactivation air fan, (F) direct evaporative cooling, (G) reactivation energy source, (b) Chart of psychometric processes [20]

3. The Functionality of a Traditional Cooling Structure

3.1. A framework of the case study

An FCU for a lecture hall erected on the second floor of the construction at the Technical Institute-Suwaira, Middle Technical University, Baghdad, IRAQ, positioned at 2◦ 55′ 13.0″, was selected as a case study for the first stage in the electricity management procedure. As shown in Fig. 6, this study was divided into FCU boundaries and a space barrier. The chilling water source (CHWS), chilling water returns (CHWR), chilling coil, devotee, and four air passageways (offer, exchange, new, and mix) are all located along the FCU borders.

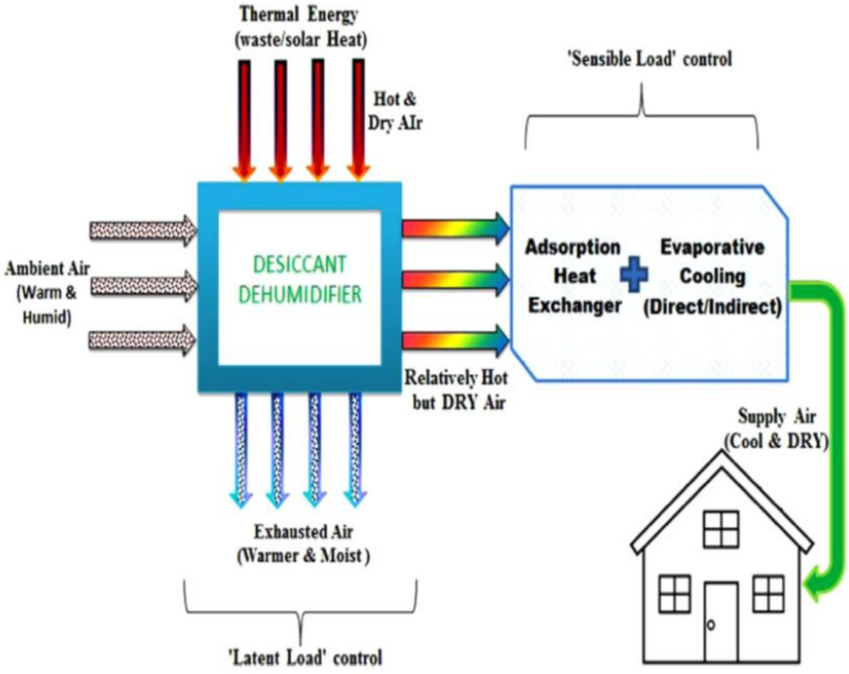

Fig. 6. Bounds of the case study

Features of the lecture room: The 24 m^2 space is used for academic sessions and seminars for 30 participants. The lecture room is surrounded by two interior (B and C) and two exterior (A and D) walls. Walls A, B, C, and D are oriented as follows: the south, north, north, and the south, in that order (Fig. 8). 97% of the space is made up of windows, and the stairs are located in the center of Wall A (Fig. 8). The two entry doors of the area are located on Wall B, also known as the hallway wall. Wall C is a partition shared by the examined room and the adjacent room. The direction, kind, and dimension of the room's partitions, windows, and gates affect heat gain; Table 1 provides specifics on these features. The U-value of exterior walls comprising 15 cm thick cement mortar and brick was 2.24 W/m2K. It is necessary to identify the room's current technology to calculate the cooling demand. The space has one 130-watt data screen and 16 additional 60-watt fluorescent light bulbs [27].

Table 1. The room specification

Subject	Dimension (cm)			Type	Material	U-value (W/ m^2K)
	Length	Width	Thickness			
Wall A	790	283	16	External wall	Brick plaster	2.35
Wall A	790	283	16	Internal wall	Brick plaster	2.35
Wall A	790	283	16	Internal wall	Brick plaster	2.35
Wall D	790	283	16	External wall	Brick plaster	2.35
Ceiling	790	652	38	Poorly insulated	Cement Concrete	1
Floor	790	652	38	Poorly insulated	Cement Concrete	1
Window	580	290	1	Single glazed	Glass	5.8
Doors	215	148	6	Swing door	Wood	3.08
Shades	580	290	0.3	Sliding panels	fabric panels	-

Features of a fan coil unit: A 17.5 kW FCU with dimensions of 429 mm × 899 mm × 1475 mm, an overall water velocity of 2592 kg/hr, and an overall capacity was mounted on the lecture room ceilings. The transfer of warmth in the cooling system occurs in the FCU through an airflow/water circulation mechanism. The air-water flow process in the FCU, which is implicated in the particular research's boundary, is depicted in Fig. 7. The heat that is sensible from the room is transferred to the water that circulates in the cooling system by a combination of the returned air (red) and clean air (green). Following the electrical drying and decrease in temperature procedure of the chilling coil, six diffusion devices disperse the blue air source throughout the space. The fan, pumps, and compressor were identified as the FCU's energy-intensive parts. The fan unit consists of a 2 kW DC motor and a rotor. By calculating the cooling system's capacities (kW) and hydraulic horsepower (kW), the energy expenditure of the pumps and chilling was measured [28].

3.2. FCU energy audit

Administrators can enhance the sustainability of a structure and assess its energy use through energy audits [29]. In this research, the energy consumption of a lecture room was evaluated using three ASHRAE energy auditing levels. Level 1: Site evaluations, sometimes referred to as initial inspections, include an overview of the building's electrical system and can assist in locating information required to study energy consumption [30]. An initial study was conducted to better understand how to distribute energy in a structure. The research included a review of the site's operating data and power bills, which showed that the FCU system is the main energy consumer in the lecture room.

Further inspection revealed that the lecture room's outside temperature was significantly below what the people inside could tolerate for warmth, forcing them to dress warmly. The substantial electrical power use of the cooling system to achieve the proper humidity level in the lecture room is the cause of the observed excessive cooling. Consequently, mechanical drying in FCU devices is responsible for significant energy usage in a building. A comprehensive plan has been presented to modify and enhance Iraq's traditional building conditioning methods in the wake of the initial evaluation. Therefore, cost reductions could be achieved by replacing the conventional cooling and drying procedures in a building's climate control system.

A thorough investigation of the suggested cooling systems is necessary before creating the methods for conserving energy. A comprehensive energy audit by ASHRAE Level 2 entails analyzing energy usage in-depth and determining energy-saving strategies [31]. In the meantime, level 3 inspection includes data collection, technical evaluation, and surveillance. These were used as a reference for figuring out how much energy was allocated precisely in the suggested cooling systems. According to the investigation limitations, FCU's performance was assessed in this study. The necessary measurement variables and their corresponding positions within the case study boundaries have been determined, as indicated in Table 2. The perceptive and implicit load of the area, as well as variations in heat retention, were observed at the chamber's boundaries.

Three major parts make up the FCU boundaries: a fan, a circulation device, and a chiller. To determine the overall energy of the FCU, the energy usage of each element was monitored and documented. Since one particular fan is attached to a matching FCU, the power utilization of the fan can be directly measured using a fan key. The cooling coil's capacity of the chillers, which is determined by the air qualities of all four air channels—fresh air, combined air, provided air, and return air—was used to calculate the energy the device utilized. In the meantime, the cooled water velocity was used to calculate the pump's energy usage.

Every piece of surveillance equipment, such as climate and humidity detectors and water and air circulation meters, was placed where it needed to be, as Fig. 7 illustrates. Every piece of gear was linked to a data logger's channels to log data using a PC. The data recorders were set up to gather data every 20 minutes between the hours of 8 AM and 6 PM. Personal measurements were taken to verify the accuracy of the deployed supplies, wiring, system, and data recorder results. Throughout data collection, the FCU system remained operational. The FCU was set at 25°C, which is recommended for indoor temperatures according to ASHRAE standards. The circumstances of the space and FCU were constant during the six-month data-gathering session. To evaluate the demand for cooling, FCU efficiency, and case study simulation verification in TRNSYS, the collected data were examined.

4. Performance of Solar Desiccant Cooling Systems

4.1. Simulation study of the proposed desiccant cooling systems

This work has hypothetically examined the efficiency of three solid dehumidifier drying cooling equipment designs: TSDCS-V, TSDCS-R, and HDSC, utilizing the TRNSYS application. The solid desiccant wheel (DW), heat recovery wheels (HRW), heat exchanger (HX), solar array to replenish the desiccant, and cooling segment (direct evaporative (DEC) or VC) are the main parts of a dehumidifier cooling system. Fig. 9 displays the arrangement and simulation models. To evaluate the adiabatic (two-phase) dehumidifying method in Iraqi tropical weather, the TSDCS-V and TSDCS-R simulations were selected [32]. The air management systems of the two versions are different despite the elements being nearly the same. The performance of an integrated dehumidifier system for cooling in Iraq's climate was examined using the prototype HDCS. Dehydration ability, which is the proportion of humidity removed from the air through the dehydration process, is the main difference

among single-stage and two-stage systems. The regenerated temperatures can be found throughout the entire simulation by altering and establishing the required humidity ratio following dehydration in the DW (moisture ratio set position). The air conditioning system's dehydration threshold was changed to 0.010 kg/kg using a one-stage dehumidifier wheel. The moisture ratio established for the first and secondary DWs in two-phase airflow and looping modes correspondingly 0.0100 kg/kg and 0.0050 kg/kg. All models have two air lines: the recuperation side discharges ambient air to the outdoors through a method, and the procedure side gives supply air. Important components of the procedure and rejuvenation side were highlighted by numerals to identify the characteristics of air [33].

V and R in TSDCS: Two DWs, two heat recuperation tires, two evaporative air conditioners of different abilities, two warmth exchangers, two supplemental furnaces, and a vacuum-tube collector make up the multi-stage granular cooling structure (Fig. 7). The velocity of airflow on the regenerating side was 1160.5 kg/hr, whereas the rate of airflow on the procedure's side was 2321.1 kg/hr. Two-step dehydration in the DWs (2 and 4), two-step pre-cooling in the heat-recovery wheels (3 and 5), and a single-step chilling in the direct absorption cooler (6) are the procedures that provide the supply air for the procedure's side. The surrounding air (8) and incoming air (7) are combined on the fresh air side before being cooled in one direct evaporation cooler. After that, the evaporation cooler's (9) outgoing air is divided into two stages, each with an equal circulation rate. At every step (12 and 15), the air is warmed in the heat recuperation wheel (10 and 13), cooled by solar-powered heaters (11 and 14), and then humidified in the DWs. HDCS: Fig. 8 shows a schematic representation of the hybrid dehumidifier cooling structure. The main parts of this equipment system are a drying wheel, a thermal recovering wheel, a direct evaporation chiller on regenerating each other, and a cooling coil that functions on the procedure front. After chemical dehydration (1-2), the surrounding air gets cooled by the thermal recuperation wheel (2-4) and then by the cooling unit (3-5). The cooling coil, which can accumulate much less than the FCU, is where physical dehydration occurs. The hybrid technique's regenerative and manufacturing sides had airflow rates of 2321.1 kg/hr. The effectiveness of the suggested models (Fig. 9) when used as the alternate air conditioner to the FCU for the lecture hall was simulated using the TRNSYS 16 application. The primary modeling elements utilized in the TRNSYS application are shown in Table 3.

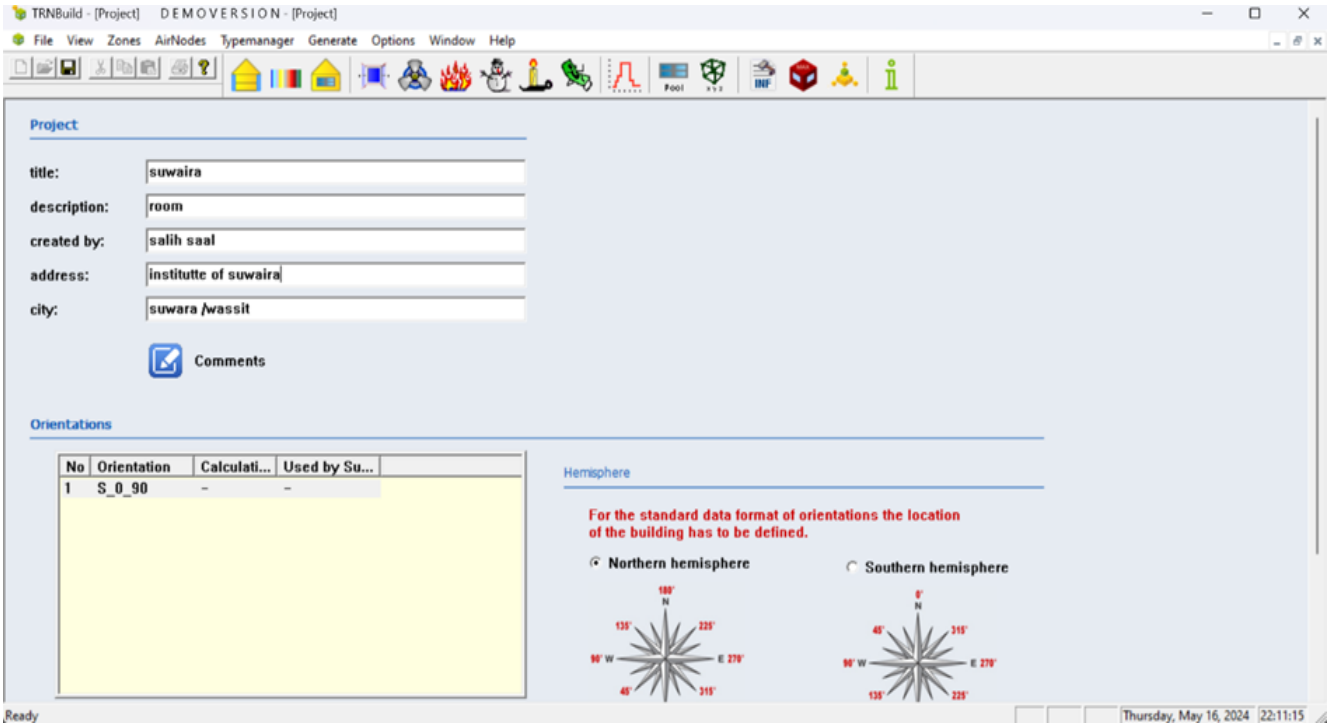

Fig. 7. The main window of TRNSYS 17

Table 2. The main TRNSYS components for simulation

Type of components in TRNSYS	Name of the main component	Properties
Type 683	DW	F1 = 0.1, and F2 = 0.08, speed of rotation: 8 r/h
Type 683	DEC	saturation efficiency = 0.9
Type 683	HRW	sensible efficiency = 76.6%, latent efficiency = 0%, power consumption: 0.18 kW
Type 683	HX	Effectiveness = 0.8, the specific heat of the hot side is 4.23 kj/kg.K, and the specific heat of the hot side is 1.07 kj/kg.K
Type 683	Pump	maximum power consumption: 60 W, water flow rate: 170 kg/h
Type 683	Blower	motor efficiency = 0.86, maximum air flow rate: 2431.1 kg/h
Type 683	Room (load)	TRN build, input data: Table 1, and measurement data
Type 683	Weather data	all of the weather data is based on Technical Institute Suwaira
Type 683	Solar collector	evacuated tube, area of collector: 25 m2, The efficiency of the collector η: 0.78
Type 683	Hot water tank	The loss coefficient: 0.58 W/m² K

Table 3. Simulation and measurement of the average air characteristics of the FCU-Room

Situation of air Temperature (°C)	Temperature (◦C) simulation	measurement	Δ	Humidity ratio (kg/kg) simulation	measurement	Δ
Room air	24.58	25.11	-0.8	0.0157	0.0153	1.47
Mix air	24.44	25.24	2.42	0.0167	0.0173	4.43
Supply Air	18.57	18.63	1.4	0.0123	0.0121	2.63
Outdoor air	28.32	28.42	1.5	0.0194	0.0196	2.3

4.2. Verification

The classroom design (52a) for the created TRNSYS modeling was verified using the actual study measurements and the area's attributes. In the meantime, a test environment was used to evaluate the simulation's dehumidifier conditioning components. Verification of the space simulation (52a): To confirm the classroom framework, an FCU-TRN Build simulation was created and generated in TRNSYS using information gathered from the electrical auditing. The necessary data, including setting, wall and frame introductions, ground and roof requirements, coloring, and room attributes, have been entered into TRN Build frames according to the features of the case study boundaries. Measurements of humidity levels, solar radiation, and outside temperatures have been made to provide the necessary data for the simulations. TRN build's production has been adjusted for hidden demand on cooling and perceptible cooling. To verify the precision of the modeled lecture room, the outcomes of the case investigation simulations and measurements (energies audit) about cooling demand and air properties were contrasted. Fig. 10 illustrates the difference in conditioning demands between the measurement and modeling data. The perceptible load had a variation of 2.9%, while the entire cooling load had a variance of 2.9%. The hidden burden was the most unique, with a variation of 3.5%. The significant impact of penetration on dormant load is explained by a variance in chilling load, which is likely related to the discrepancy between prediction and measurement results of weather information. Based on modeling and measurements, Table 3 displays the mean moisture and temperature values recorded at different stages throughout the case study. Variations in temperatures between simulations and measurements were found to be between –0.9% and 2.31%, as well as between 1.35% and 4.32% for the humidity ratio. The most notable differences were the air temperatures and moisture mix brought on by clean air (surrounding climate circumstances).

Verification of evaporative cooling elements through practical configuration: At Iraq's Solar Technological Park, a solar-powered dehumidifier cooling structure was constructed next to the test facility. Fig. 10 depicts the simulated configuration of the test room's supplied air circulation apparatus. The cooling demand in the examination hall was changed to correspond with that in the lecture hall. Three fundamental parts made up the implemented system were as follows: The chilling unit included three heat resources: a) a solid dehydrator wheel with silicone gel as an absorber; b) evacuation tube collectors and supplementary warmers; and c) a heat recuperation wheel and an immediate evaporation chiller. An electricity burner is installed as a backup heater for overcast days, and a 25 m² sunlight evacuation tube is used to generate warm water with temperatures in the range of 80–120 °C. The blower engine and the electrical heater used about 150 and 1500 W of power, respectively. Table 3 contains a list of the constituent specs. Sensors for moisture and temperature were installed at the nine predetermined locations in the overall established to identify the air condition. The instruments were connected to the ADAM data collection system, which was used daily from 8 a.m. to 6 p.m. for one month to collect the necessary data. The collected moisture and temperature proportions from the practical and simulated settings were contrasted at nine specified points, as illustrated in Fig. 8. The difference between the empirical and simulated values was 6.5% and 1.3%, respectively. The computer model of the dehumidifier cooler was therefore verified, resulting in a mismatch between the simulated and empirical findings of 6.5 percentage points.

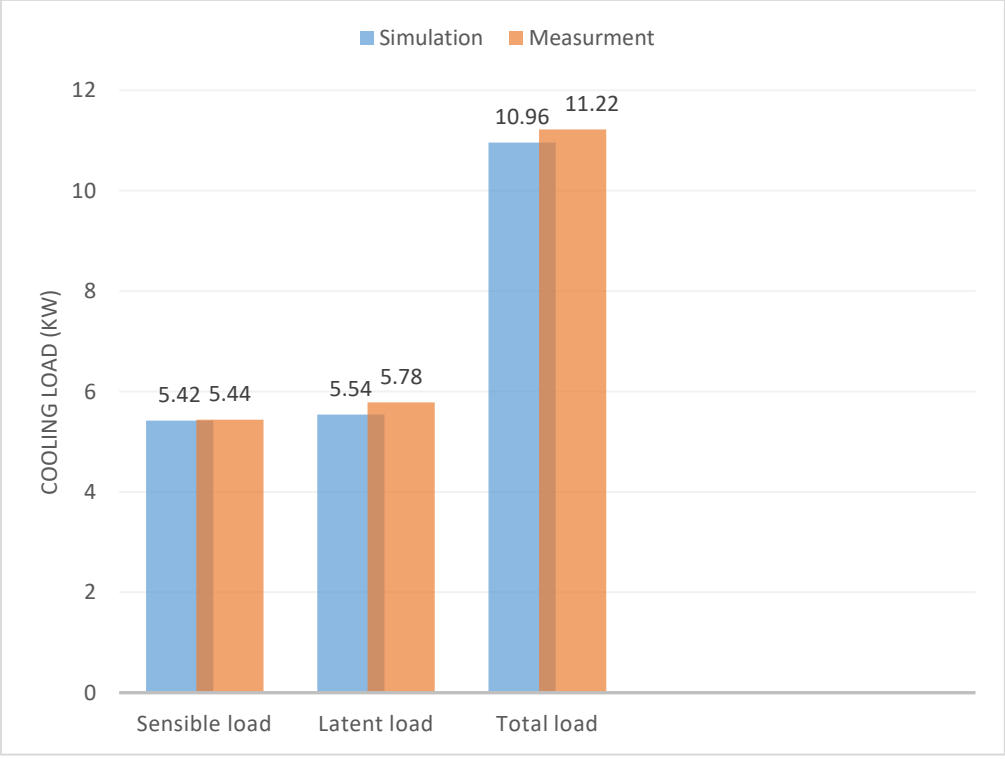

Fig. 8. Validation of seminar room model by cooling load

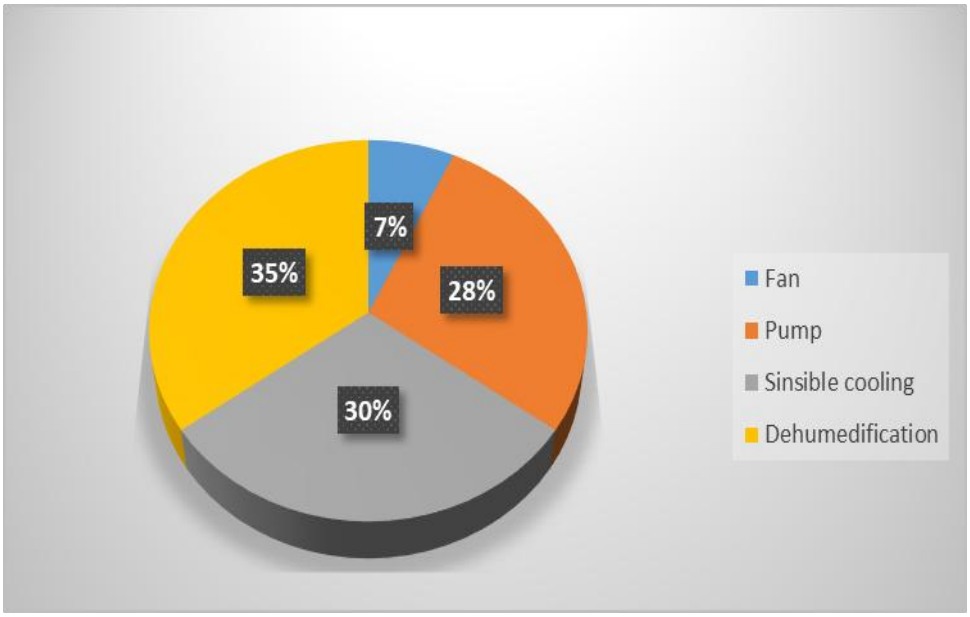

Fig. 9. Apportioning of energy consumption in FCU

5. Results and Discussion

5.1. FCU energy usage

The temperature and efficiency allocation have been examined regarding the case study's (FCU-room) efficiency following data acquisition through an energy inspection. Visible and hidden loads were identified for 10 hours daily, from Monday through Friday. The findings indicate that the hidden load (51%) was greater throughout the week than the apparent load (49%). The mean quantities of hidden and perceptible loads were 50 kWh and 40 kWh, respectively. The internal environmental situation of the space was evaluated using the moisture level, temperature, and airflow velocity at designated case study points. The average temperatures, humidity proportion, and airflow rate at various FCU locations throughout a 200-hour operation are displayed in Table 4. The outside, hybrid, provided, and chamber (return) air quality is represented by the numbers 1, 2, 3, and 4. The temperature and moisture ratios of the provided air (point 3) were 17.8 ◦C and 92.9%, respectively, whereas those of the space's air (point 4) were 24.3 ◦C and 77.2%. The ASHRAE comfortable conditions state that interior conditions should be designed with a moisture content of 50%, an ambient temperature of 25 °C, and a moisture ratio of 0.0098 kg/kg. Because the lecture room's moisture content (77.2%) was greater than 50%, it could not attain a comfortable temperature with the FCU.

The entire energy utilized by the three evaluated FCU components—the fan, pump, and chiller—is included in the FCU's electrical consumption. The mean electrical usage of every cooling element from Monday through Friday is displayed in Fig. 10. Throughout the week, the air conditioner uses between 35 and 45 kWh of electricity. The energy usage of the fan and pump is almost constant at 4 kWh and 16 kWh, respectively. The overall energy usage of FCU varies between 58 and 66 kWh on a Monday through Friday basis. The chillers, pumps, and fans accounted for 66%, 27%, and 7% of the total energy usage, according to FCU's energy dividing. It was discovered that the chiller accounts for a significant amount of energy consumption, while the fan only accounts for a minor percentage. The majority of the energy used by the FCU is used by the chiller component. Therefore, by concentrating on the chillers, we can pinpoint the chiller area with considerable potential for energy reduction. The chiller system generates cold water to facilitate dehumidifying and practical cooling procedures in the conditioning coil. Nonetheless, the chiller's energy usage results in the cooling coils using its two functions—dehumidification and sensible cooling. As a result, the chiller's energy usage can be divided into two categories: perceptible cooling and dehumidifying.

Fig. 9 clarifies the energy distribution in various regions of the FCU, enabling the identification of possible energy savings. The dehumidifying manipulations, practical cooling-down pumps, and fans contribute 37%, 29%, and 7% of the total energy used. The power allocation in the FCU shows that at 37% of the total energy utilized, drying represents the largest portion of the electricity used in the FCU. The average energy consumption for each FCU process on a daily, weekly, and monthly basis is shown in Table 4. The results reveal that, at 22.8, 117.4, and 454.63 kWh, the dehumidifying procedure uses the most power on a daily, weekly, and monthly schedule. Given Iraq's hot and muggy conditions, a significant amount of energy is needed to dehumidify the FCU mechanically. Thus, the potential for energy savings might be assessed by substituting chemical drying with hydraulic dehumidifying.

Table 4. Air properties of seminar room under FCU operation

No	Point	Temperature (◦C)	Humidity ratio (kg/kg)	Relative humidity (%)	Airflow rate (kg/ hr)
1	Room air	29.5	0.0300	77.9	474.22
2	Mix air	25.8	0.0173	78.1	2421.1
3	Supply Air	18.6	0.0129	93.9	2421.1
4	Outdoor air	24.8	0.0158	78.2	1846.88

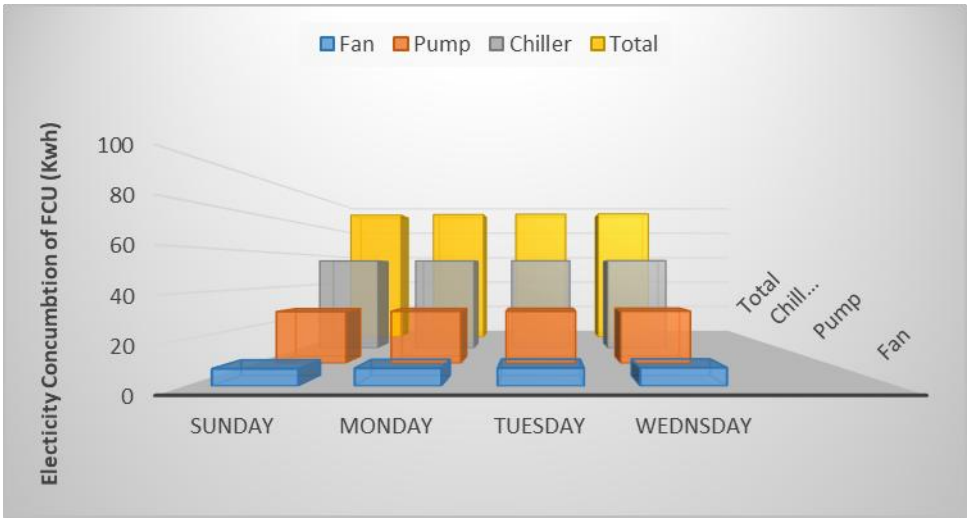

Fig. 10. Energy consumption of FCU

5.2. Simulation results

The outcomes of 200 hours of computations using the suggested models in a lecture hall (case study) are shown in this section. The simulation findings of the suggested models were examined using performance measures described in the following sections, including thermal convenience, COP, solar fractions, and energy efficiency.

5.2.1. Thermal condition analysis of the room under desiccant cooling

The parametric charts for the suggested models are shown in Fig. 9. These charts were created utilizing the air attributes (the mean degree Celsius and humidity ratio) at particular simulation installation points. The process-air and regeneration-air sides are indicated by red and blue paths. TSDCS-V model: The results of both the initial and second drying processes are shown in Fig. 11, where the moisture content of the air percentages was 0.0100 as well as 0.0050 kg/kg, correspondingly. The initial reproduction occurred at around 70 ◦C, while the second occurred at about 76 ◦C. Point 6 showed the moisture content and temperature of the supply air at 18.6 ◦C and 71.2 %, respectively, whereas Point 7 showed the room temperatures and percent moisture at 25.5 ◦C and 61.9%, respectively. While the room temperatures and percent humidity (such as point 1) were 25.1 ◦C and 65.3%, accordingly, the supply air temperature and relative humidity (point 6) in prototype TSDCS-R (Fig. 11) were 18.3 ◦C and 75%, correspondingly. The air's moisture percentages became 0.010 and 0.0050 kg/kg following the initial and secondary dehumidifications. The initial and second regenerations occurred at degrees close to 75 °C. Fig. 11 displays the composite dehumidification cooling method's calibration curve. The average temperature increased to 54 ◦C, and the proportion of humidity was dropped to 0.010 kg/kg by a one-stage drying operation (air process from point 1 to point 2). The reading was lowered to 29 °C while the relative humidity stayed the same in the heat recuperation wheel (point 3). The moisture ratio and supply air temperature were reduced to 0.007 kg and 18.3 ◦C, respectively. Type HDCS might supply the lecture hall with the right amount of supply air by integrating an electrical dehydrating procedure in the cooling fan with an electrical dehumidifying operation in the DW. The lecture room was overcooled in section 2 of the ASHRAE energy assessment level 1 due to the FCU coil's thorough cooling to meet the latent load. Therefore, before using any of the suggested dehumidifier cooling systems, it is imperative to analyze the space's temperature conditions (degrees Celsius) and percent moisture. The following subsection assesses the lecture room's temperature conditions using a simulation performed in TRNSYS using the three dehumidifier conditioning system simulations used as the cooling system's components. The environmental conditions of the lecture hall might reach a comfortable thermal state (25 ◦C, 50%, 0.099 kg/kg) when the ventilation system generates supplied air between an acceptable range of 18.3 ◦C and 0.007 kg/kg, according to the ASHRAE standards and the cooling demand of the case study.

Because of the varying amounts of provided air that the cooling mechanisms create, the simulation shows that implementing various conditioning techniques in the lecture room results in varying realized indoor temperatures and humidity levels. Figs. 11 and 12 display the moisture and temperature recorded in the lecture room over 20 working days when various dehumidifier cooling devices and the FCU were applied. Figs. 11 and 12 show that while the room temperature in model TSDCS-V is around 1 ◦C higher than 25 ◦C, it is close to 25 ◦C in designs TSDCS-R, HDCS, and FCU. The design of the HDCS was discovered to reach a relative humidity that was almost 50%, making it the best-performing model out of all the others. With the other variants, TSDCS-V and TSDCS-R, the room's relative moisture could be reached between 61% and 66%. As a result, in Iraq's tropical climate, where temperatures of 25 °C and a moisture content of 50% are necessary for the training room, the simulation of HDCS is theoretically possible for space conditioned with high sensing and lateral cooling demands (reasonable load: 49%, Lateral load: 51%). Thus, areas with a latent load of under 51% or where the moisture content is suitable within a limit of 61%-66% may be able to implement the TSDCS-V and TSDCS-R systems.

5.2.2. Solar fraction analysis of the desiccant cooling systems

Poor-quality (heat) power is used for most of the power in a dry cooling structure, enabling connection with solar thermal power. Consequently, the drying wheel was regenerated using sunlight in the suggested arrangement designs, decreasing its power usage and improving the COP efficiency of the device. An additional heater powered by solar energy was used as an emergency heat source for regenerating activities to guarantee proper cooling efficiency. For twenty-seven days of work in December 2022, the sun energy in Iraq is shown in Fig. 13. The smallest and maximum amounts of ultraviolet (UV) rays are 15.11 MJ/m^2/day and 28.12 MJ/m2/day, respectively. This indicates that sunlight is essential to power preservation and dry refrigeration systems. Sunlight fraction (SF) is the proportion of sunlight to the total power needed for renewal. For every possible type suggested, the TRNSYS simulations maintained a constant quantity of incoming sunlight and, consequently, the heating

output of the solar collector. As a result, the amount of sunlight used in an air conditioner is determined by the energy needed for solid adsorbent regeneration. Fig. 13 displays the changes in solar percentage for each of the three simulations over twenty consecutive days of work. Designs with an elevated solar percentage regenerate with less thermal energy. Since one-stage dehydration uses less regenerating energy than a two-phase dehumidifying system in venting mode, simulation results revealed that the SF of the HDCS versions are higher than that of the TSDCS-V versions. In the meantime, the HDCS version has the highest SF (0.61), while the TSDCS-V design has the smallest SF (0.57).

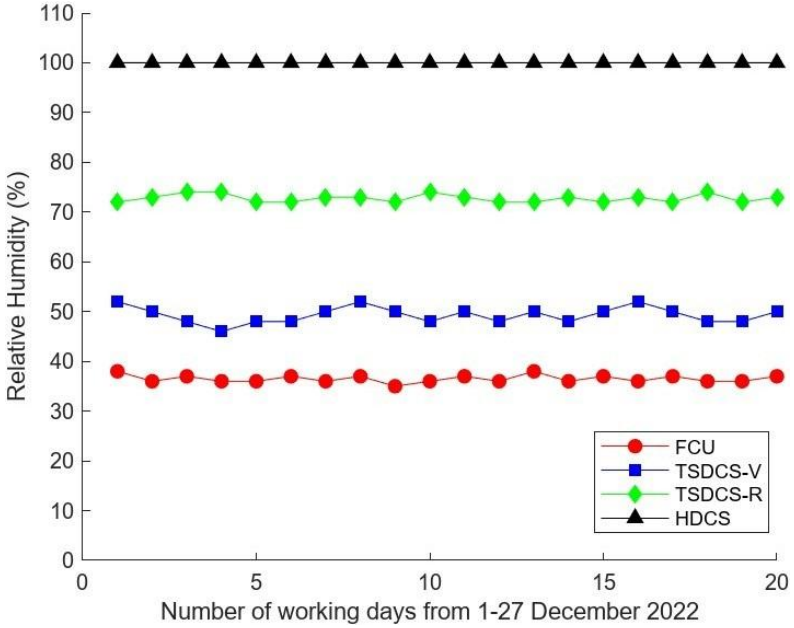

Fig. 11. Relative humidity of seminar room provided by different models

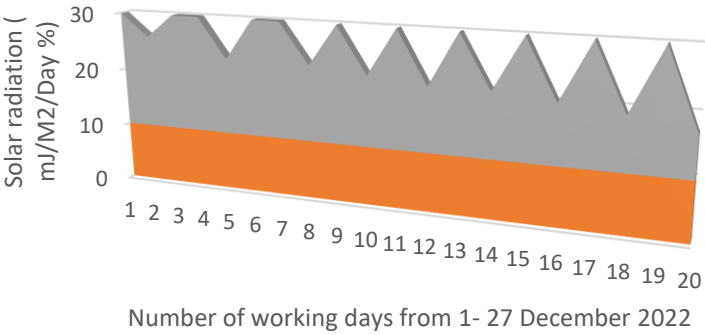

Fig. 12. Solar radiation in Iraq for 20 working days

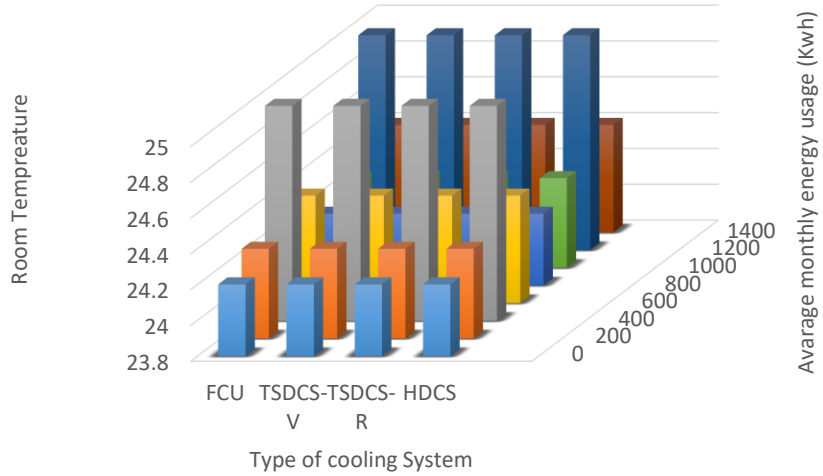

Fig. 13. Comparison of average monthly energy usage and room temperature in different models

5.2.3. Energy consumption analysis of the desiccant cooling systems

This section included three analyses of the generated designs: constituent overall allocation, energy utilization over time, and overall energy use. The parts of a dry cooling unit that require the most power are the DW, HRW, supplemental furnace, and DEC. In comparison to FCU, Fig. 14 illustrates how power is allocated to the major components of evaporative cooling structures according to typical daily energy usage. With 24.86 kWh (56%) used by the spare heater, the version TSDCS-V used the most power. Other energy-consuming components included the fan, HRW, DEC, hot water pumps, and DW, with corresponding energy consumption of 8.12 (18%), 7.4 (17%), 2.5 (6%), 1.5 (3%), and 0.186 kWh (0.04%). The capacity for dehydration is closely correlated with the regeneration temperatures and the energy consumption of the backup heaters. Type TSDCS-R's decreased capacity for drying resulted in a 21.2 kWh energy use reduction for the auxiliary heater. Version TSDCS-R and design TSDCS-V shared comparable energy-intensive parts. Compared with the HDCS, the TSDCS-V and TSDCS-R versions utilized more energy for DW and HRW due to their two-phase dehumidifying and heat recuperation processes. With daily energy consumptions of 21.1 and 17.27 kWh, the secondary heaters and the cooling mechanism of the vacuum cleaner (VC) are the two major energy users in the HDCS. In FCU, the cooler used 41 kWh of power, double the amount of the desiccant cooling systems and their standby heaters. The electrical power usage of the reported FCU and the simulation's models over twenty days of work in a month is shown in Fig. 14. The findings show that HDCS's electrical usage trend was between 48.04 and 52.6 kWh, with the suggested models having the greatest average per day electrical use of 50.99 kWh. The FCU uses a median of 61.86 kWh daily, ranging from 57.3 to 71.5 kWh. In the meantime, the daily averages for the TSDCS-V and TSDCS-R models were 44.57 and 40.89 kWh, respectively, and ranged from 40.1 to 46 and 39.1 to 45.7 kWh, respectively. When determining the most effective model, energy efficiency and the state of the room's temperature are crucial performance gauges. The median monthly amount of total energy use and ambient temperature for every variant of the FCU is shown in Fig. 14. Versions HDCS, TSDCS-V, and TSDCS-R used 1019.7, 891.3, and 817.8 kWh of electricity per month, accordingly, to maintain a pleasant ambient climate within 25 and 25.5 ◦C. Based on the measurements, the FCU used 1237.26 kWh each month to keep the room temperature between 24.4 and 24.6 ◦C. Therefore, suggested approaches could substitute FCU with large savings in energy by contrasting the performance of dry air conditioners and FCU concerning comfortable temperatures and monthly energy utilization.

5.2.4. Energy-saving potential of the desiccant cooling systems

The cost-effective proportion and decrease in carbon dioxide emissions for each dehumidifier type used in the lecture room's air conditioning system are displayed in Fig. 14. It has been demonstrated by simulations that each design has a distinct energy consumption, which leads to a variation in the possibility of energy savings (PES). The computational research indicates that the TSDCS-R version is particularly energy-efficient, conserving 419.5 kWh (33.9%) monthly. Versions TSDCS-V and HDCS, on the other hand, save 346 (27.9%) and 217.3 (17.27%) kWh, correspondingly. However, given the feasible ambient temperature spectrum inside the comfortable thermal conditions when used in the lecture room, every model provides an adequate possibility of energy savings. Because of its connection with a VAC structure, this kind of HDSC saves little power, but its moisture level and ambient temperature are optimal for thermal convenience. The opportunity for reducing CO2 emissions in the lecture room was evaluated using multiple dry cooling techniques. CO2 is released into the environment when producing power from fossil fuels. Therefore, it is advantageous to the natural world and potentially environmentally friendly to utilize energy-efficient models since energy reductions could reduce emissions of greenhouse gases. The computational findings show that significant amounts of carbon dioxide (CO2) can be avoided in the lecture hall by implementing a desiccant air conditioner. With monthly values of 256.4 kg and 495.01 kg, accordingly, the HDCS and TSDCS-R models produce the smallest and highest levels of gas reductions in emissions.

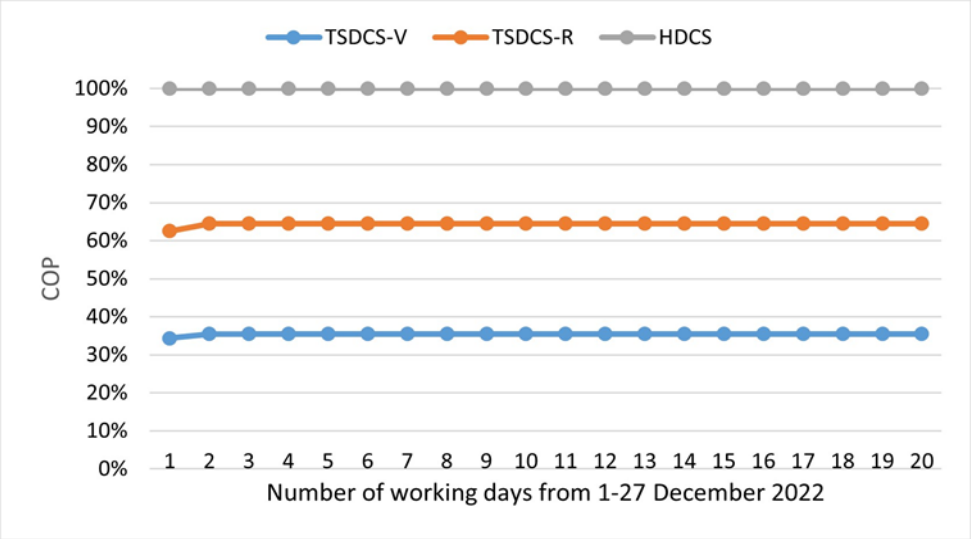

Fig. 14. COPs of desiccant cooling systems

5.2.5. Analysis of desiccant cooling system performance

The capability of cooling and the quantity of power needed for regenerating are the two parameters that decide each algorithm's COP. The variations in temperatures between the atmosphere before the drying wheel and the provided air in the treated air cause the cooling capabilities of the HDCS, TSDCS-V, and TSDCS-R models to change. The suggested models' efficacy during twenty hours of work is shown in Fig. 14. An elevated COP can be achieved by the design with the greatest cooling capability and the least amount of regenerating power. Design TSDCS-V has the greatest COP compared to the other designs, while Type TSDCS-R has the smallest. The TSDCS-V version achieved a COP of 1.16, whereas the HDCS and TSDCS-R models had COPs of 0.84 and 0.54, respectively. By evaluating the COPs between the HDCS and TSDCS-V designs, it can be seen that the hybrid dehumidifier cooling method's capacity for cooling and COP is increased when VC is used. The two-

stage dehydration process of TSDCS-V affects COP more than the DEC due to its larger effect on temperature drop. Measurements of TSDCS-V/TSDCS-R COPs showed that switching the airflow mode to recirculating in two-phase devices decreases the COP value. The cooling power and temperature drive decrease, with the chilling power trend becoming more prominent than the temperature drive development, leading to this loss.

6. Conclusion

- This study investigates and designs a solar-powered air heater using vacuum tubes numerically, starting with model creation and meshing, followed by implementing boundary requirements.
- After performing an electrical analysis, conditions, heat flow, and heat exchange data were examined, indicating that a reduced collecting surface is required as the incoming flow to the collector improves, enhancing overall effectiveness.
- Less energy loss results in a smaller sensor area requirement, dependent on the barrier's thermal conduction ratio; a thicker barrier reduces the necessary collecting area.
- Alterations in the collector's sectional area have been shown to increase heat transmission efficiency, where heat absorption causes the collector's sectional shapes to shrink, thus raising heat exchange velocity.
- The study compared the efficiency of three different dry cooling structures (TSDCS-V, TSDCS-R, HDCS) with an FCU in a seminar room, using energy audits to assess the FCU's efficiency in terms of insulation and energy allocation.
- TRNSYS modeling and laboratory configuration confirmed the properties of dry cooling structures, with significant findings from the FCU energy audit indicating the lecture room's moisture content (77.2%) was too high for warmth under FCU conditions.
- The dehydrating process at the FCU consumed the most energy (37%), with yearly, weekly, and monthly averages of energy use being 22.8 kWh, 117.4 kWh, and 454.63 kWh, respectively.
- The dehydration procedure is determined to be an essential part of the refrigeration system, suggesting potential energy savings through chemical dehumidifiers over conventional methods.
- HDCS is found to be functionally feasible for space conditioning in a lecture hall under Iraq's tropical climate, requiring a room temperature of at least 25 °C and 50% moisture content, as verified by TRNSYS simulations.
- Temperature and moisture content in the room could be maintained closer to 25 °C–25.5 °C and 61%–66%, respectively, using TSDCS–V and TSDCS–R.
- Such simulations could be practical in conservatories or spaces with low latent loads where a relative moisture level of 61–66% is appropriate.
- Among the three models, TSDCS-R achieves the highest monthly energy savings at 419.5 kWh (33.9%), followed by TSDCS-V and HDCS with 346 (27.9%) and 217.3 kWh (17.27%), respectively.
- TSDCS-V and HDCS result in the smallest and highest gas emissions reductions, with monthly averages of 256.4 kg and 495.01 kg, respectively.
- Type TSDCS-V achieved a COP of 1.16, while models HDCS and TSDCS-R recorded COPs of 0.84 and 0.54, respectively.
- The HDCS model shows the highest SF (Solar Fraction) of 0.615, followed by TSDCS-R and TSDCS-V with 0.61 and 0.57 SF, respectively.

Acknowledgment

This work is partially supported by the Department of Mechanical Engineering, South Tehran Branch, Islamic Azad University, Tehran, Iran, and the Department of Mechanical Engineering, Kermanshah Branch, Islamic Azad University, Kermanshah, Iran. Thanks to the Ministry of Higher Education & Scientific Research, Iraq, and the Middle Technical University, Iraq.

References

[1] T. Yu, P. Heiselberg, B. Lei, M. Pomianowski, and C. Zhang, "A novel system solution for cooling and ventilation in office buildings: A review of applied technologies and a case study," Energy Build., vol. 90, pp. 142–155, 2015. https://doi.org/10.1016/j.enbuild.2014.12.057

[2] R. Vanaga, A. Blumberga, R. Freimanis, T. Mols, and D. Blumberga, "Solar facade module for nearly zero energy building," Energy, vol. 157, pp. 1025–1034, 2018. https://doi.org/10.1016/j.energy.2018.04.167

[3] M. Carrasco-Tenezaca et al., "Effect of passive and active ventilation on malaria mosquito house entry and human comfort: an experimental study in rural Gambia," J. R. Soc. Interface, vol. 20, no. 201, p. 20220794, 2023. DOI:10.1098/rsif.2022.0794

[4] U. Stritih, P. Charvat, L. Klimes, E. Osterman, M. Ostry, and V. Butala, "PCM thermal energy storage in solar heating of ventilation air—Experimental and numerical investigations," Sustain. cities Soc., vol. 37, pp. 104–115, 2018. https://doi.org/10.1016/j.scs.2017.10.018

[5] B. Purushothama, Humidification and ventilation management in the textile industry. Crc Press, 2024.

[6] A. G. Kehbila, R. K. Masumbuko, M. Ogeya, and P. Osano, "Assessing transition pathways to low-carbon electricity generation in Kenya: A hybrid approach using backcasting, socio-technical scenarios and energy system modelling," Renewable and Sustainable Energy Transition, vol. 1, p. 100004, Aug. 2021, doi: 10.1016/j.rset.2021.100004.

[7] J. S. Abdullayev and R. E. Humbatova, "Hydrogen production and reduction of carbon emissions in Azerbaijan's energy transition: challenges and prospects," Azerbaijan Oil Industry, no. 03, pp. 21–28, Mar. 2023, doi: 10.37474/0365-8554/2023-3-21-28.

[8] G. Xexakis and E. Trutnevyte, "Model-based scenarios of EU27 electricity supply are not aligned with the perspectives of French, German, and Polish citizens," Renewable and Sustainable Energy Transition, vol. 2, p. 100031, Aug. 2022, doi: 10.1016/j.rset.2022.100031

[9] Y. Yang, G. Cui, and C. Q. Lan, "Developments in evaporative cooling and enhanced evaporative cooling-A review," Renew. Sustain. Energy Rev., vol. 113, p. 109230, 2019. https://doi.org/10.1016/j.rser.2019.06.037

[10] H. Shen, X. Wen, and E. Trutnevyte, "Accuracy assessment of energy projections for China by Energy Information Administration and International Energy Agency," Energy and Climate Change, vol. 4, p. 100111, Dec. 2023, doi: 10.1016/j.egycc.2023.100111.

[11] C. A. A. Fernandez Vazquez, T. Vansighen, M. H. Fernandez Fuentes, and S. Quoilin, "Energy transition implications for Bolivia. Long-

term modelling with a short-term assessment of future scenarios," Renewable and Sustainable Energy Reviews, vol. 189, p. 113946, Jan. 2024, doi: 10.1016/j.rser.2023.113946.
[12] R. Stock, “Abolition solarities: Theorizing antiracist and anticapitalist solar energy insurrections,” Renewable and Sustainable Energy Transition, vol. 4, p. 100063, Aug. 2023, doi: 10.1016/j.rset.2023.100063.
[13] M. Kamran, M. Raugei, and A. Hutchinson, “Critical elements for a successful energy transition: A systematic review,” Renewable and Sustainable Energy Transition, vol. 4, p. 100068, Aug. 2023, doi: 10.1016/j.rset.2023.100068.
[14] J. Deng, T.-S. Wang, E. Zhu, S. Yuan, X. Liu, and X. Chai, “Dynamic Evaluations of a Scaled-Down Heat Pipe-Cooled System under Start-Up/shut-Down Processes Using a Hardware-In-The-Loop Test Approach,” SSRN Electronic Journal, 2023, Published, doi: 10.2139/ssrn.4372497.
[15] I. Shchur, V. Shchur, I. Bilyakovskyy, and M. Khai, “Hardware in the loop simulative setup for testing the combined heat power generating wind turbine,” International Journal of Power Electronics and Drive Systems (IJPEDS), vol. 12, no. 1, p. 499, Mar. 2021, doi: 10.11591/ijpeds.v12.i1.pp499-510.
[16] Z. Qi and R. Zhang, “Coordinated Scheduling of Micro-grid Combined Heat and Power Based on Dynamic Feedback Correction and Virtual Penalty Cost,” IEEE Transactions on Power Systems, pp. 1–12, 2024, doi: 10.1109/tpwrs.2023.3326066.
[17] P. Conti, C. Bartoli, A. Franco, and D. Testi, “Experimental Analysis of an Air Heat Pump for Heating Service Using a ‘Hardware-In-The-Loop’ System,” Energies, vol. 13, no. 17, p. 4498, Sep. 2020, doi: 10.3390/en13174498.
[18] T. B. H. Rasmussen, Q. Wu, and M. Zhang, “Combined static and dynamic dispatch of integrated electricity and heat system: A real-time closed-loop demonstration,” International Journal of Electrical Power & Energy Systems, vol. 143, p. 107964, Dec. 2022, doi: 10.1016/j.ijepes.2022.107964.
[19] H. Mohammadi and M. Mohammadi, “Optimization of the micro combined heat and power systems considering objective functions, components and operation strategies by an integrated approach,” Energy Conversion and Management, vol. 208, p. 112610, Mar. 2020, doi: 10.1016/j.enconman.2020.112610.
[20] L. Cioccolanti, R. Tascioni, M. Pirro, and A. Arteconi, “Development of a hardware-in-the-loop simulator for small-scale concentrated solar combined heat and power system,” Energy Conversion and Management: X, vol. 8, p. 100056, Dec. 2020, doi: 10.1016/j.ecmx.2020.100056.
[21] P. Cerutti, “[Ground Heat Exchange: closed-loop geothermal heat-pump systems, legislation and regulation, needs and opportunities],” Acque Sotterranee - Italian Journal of Groundwater, vol. 11, no. 1, pp. 99–100, Mar. 2022, doi: 10.7343/as-2022-563.
[22] M. BEZRODNY and S. OSLOVSKYI1, “Combined heat pump heating and ventilation system using heat of soil, sewage water and ventilation emissions,” Journal of Thermal Engineering, vol. 8, no. 4, pp. 466–476, Jul. 2022, doi: 10.18186/thermal.1145522.
[23] M. A. Khan and H. Gohari Darabkhani, “Technoeconomic Analysis and Risk Assessment of Deploying Micro-Combined Heat and Power (M-Chp) Systems for Domestic Applications,” SSRN Electronic Journal, 2022, Published, doi: 10.2139/ssrn.4044506.
[24] P. K. S. Tejes, G. Priyadarshi, and B. Kiran Naik, “Performance characteristics assessment of hollow fiber membrane-based liquid desiccant dehumidifier for drying application,” Applied Thermal Engineering, vol. 218, p. 119311, Jan. 2023, doi: 10.1016/j.applthermaleng.2022.119311.
[25] Y. Wang, B. Ruhani, M. A. Fazilati, S. M. Sajadi, A. Alizadeh, and D. Toghraie, “Experimental analysis of hollow fiber membrane dehumidifier system with SiO2/CaCl2 aqueous desiccant solution,” Energy Reports, vol. 7, pp. 2821–2835, Nov. 2021, doi: 10.1016/j.egyr.2021.05.010.
[26] J. K. Hong, I. Hwang, C. W. Roh, and M. S. Kim, “Performance investigation on electrodialysis regeneration of potassium formate desiccant solution for liquid desiccant air-conditioning systems,” Energy and Buildings, vol. 266, p. 112112, Jul. 2022, doi: 10.1016/j.enbuild.2022.112112.
[27] T. Wen, Y. Luo, M. Wang, and X. She, “Comparative study on the liquid desiccant dehumidification performance of lithium chloride and potassium formate,” Renewable Energy, vol. 167, pp. 841–852, Apr. 2021, doi: 10.1016/j.renene.2020.11.157.
[28] B. Cao, Y. Yin, F. Zhang, Q. Ji, and W. Chen, “Liquid desiccant-based deep dehumidifier working with a novel ionic liquid: Prediction model and performance comparison,” International Journal of Refrigeration, vol. 146, pp. 74–87, Feb. 2023, doi: 10.1016/j.ijrefrig.2022.09.033.
[29] D.-S. Jeon, “Performance Evaluation of Packed-Bed Type Liquid Desiccant Dehumidifier using LiCl Aqueous Solution,” Korean Journal of Air-Conditioning and Refrigeration Engineering, vol. 36, no. 2, pp. 65–72, Feb. 2024, doi: 10.6110/kjacr.2024.36.2.65.
[30] B. Guan, Z. Ma, X. Wang, X. Liu, and T. Zhang, “A novel air-conditioning system with cascading desiccant wheel and liquid desiccant dehumidifier for low-humidity industrial environments,” Energy and Buildings, vol. 274, p. 112455, Nov. 2022, doi: 10.1016/j.enbuild.2022.112455.
[31] X. Liu, M. Qu, X. Liu, L. Wang, and J. Warner, “Numerical modeling and performance analysis of a membrane-based air dehumidifier using ionic liquid desiccant,” Applied Thermal Engineering, vol. 175, p. 115395, Jul. 2020, doi: 10.1016/j.applthermaleng.2020.115395.
[32] D. B. Jani, “Experimental Assessment of Rotary Solid Desiccant Dehumidifier Assisted Hybrid Cooling System,” International Journal of Energy Resources Applications, pp. 5–13, Sep. 2022, doi: 10.56896/ijera.2022.1.1.002.
[33] S. Choi and S. Choi, “Desiccant cooling assisted vapor compression system: A double stage desiccant cooling cycle via evaporative condenser,” Applied Thermal Engineering, vol. 198, p. 117456, Nov. 2021, doi: 10.1016/j.applthermaleng.2021.117456.